


Climate and soil moisture content during development of the first palaeosol in the southern Loess Plateau

J.-B. ZHAO^{a,b,c} , X.-Q. LUO^c, Y.-D. MA^{d,b}, Q. ZHOU^a, B.-Q. CHEN^c & Y.-L. YUE^c

^aShaanxi Key Laboratory of Disasters Monitoring and Mechanism Simulation, Baoji University of Arts and Sciences, Gaoxin Road 1, Baoji 721013, China, ^bState Key Laboratory of Loess and Quaternary Geology, Institute of Earth Environment, Chinese Academy of Sciences, Yanxiang Road 97, Xi'an 710075, China, ^cDepartment of geography, School of Geography and Tourism, Shaanxi Normal University, Chang'an Road 199, Xi'an 710062, China, and ^dDepartment of Hydrology and Water Resources, School of Environmental Science and Engineering, Chang'an University, Yanta Road 126, Xi'an 710054, China

Summary

The scientific problems concerning Quaternary soil water content and the water cycle have not been researched. This study examined the soil water content and depth of distribution of gravitational water in the south Loess Plateau during development of the first palaeosol layer (S_1) by methods such as field investigation, electron microscopy, energy spectrum analysis, chemical analysis, and so on. The purpose was to reveal the climate, water balance and vegetation type at the time when S_1 developed. The depth of migration of CaCO_3 and Sr were 4.2 m below the upper boundary of the S_1 palaeosol, and the depth of weathered loess beneath the argillic horizon was 4.0 m. Ferri-argillans developed well in the argillic horizon and their depth of migration was 1 m below the argillic horizon. These findings suggest that the climate during the last interglacial was subtropical and humid, and the soil-water balance was positive. Gravitational water was present to a depth of at least 4.2 m from the top of S_1 , and the water content was adequate for tree growth. The chemical weathering index showed that this palaeosol has been moderately weathered.

Highlights

- We studied the palaeo-water content index during development of the first palaeosol.
- Soil water balance during development of S_1 palaeosol in the south Loess plateau was positive.
- Available water content was 14% during development of S_1 palaeosol.
- We suggest that a subtropical climate and forest vegetation prevailed.

Introduction

The uppermost palaeosol layer in Chinese loess deposits, the first palaeosol (S_1), is reddish-brown (7.5 YR) and formed during the last interglacial period. It developed between 125 and 75 ka (Guo & Liu, 1996) and thus formed over ~ 50 ka ago. During the last interglacial the summer monsoon strengthened (Liu & Ding, 1998; Chen *et al.*, 2006a; Peng *et al.*, 2014), precipitation increased (Sun *et al.*, 1996; Guo *et al.*, 2012), vegetation was abundant and the southern boundary of the desert moved north (Sun *et al.*, 1996). Previous studies have examined the environment under which goethite formed in the palaeosol because it can indicate large soil

water content (Jiang & Liu, 2016). However, these studies did not confirm the soil water content at this time.

Climate change on the Loess Plateau has been studied and this has provided some explanations for the periodic climate changes evident in loess strata. In addition, other research has shown both similarities and differences between the Chinese loess records and those from deep-sea sediments (Kukla, 1977; Gocke *et al.*, 2011). Loess from various parts of central Asia and Europe is also well developed, and cycles of climate change have been identified by analyses of strata from those sediments (Bronger *et al.*, 1995; Pecsli, 1997; Bokhorsta *et al.*, 2009).

Previously, age, climate, vegetation and soil properties were among the main areas of interest for those specializing in loess and palaeosol research, whereas research on soil water content and variation in the water cycle during loess deposition and soil formation have been limited. Microstructures in loess and

Correspondence: X.-Q. Luo. E-mail: luoxq0815@126.com; J.-B. Zhao. E-mail: zhaojb@snnu.edu.cn

Received 15 June 2016; revised version accepted 27 December 2017

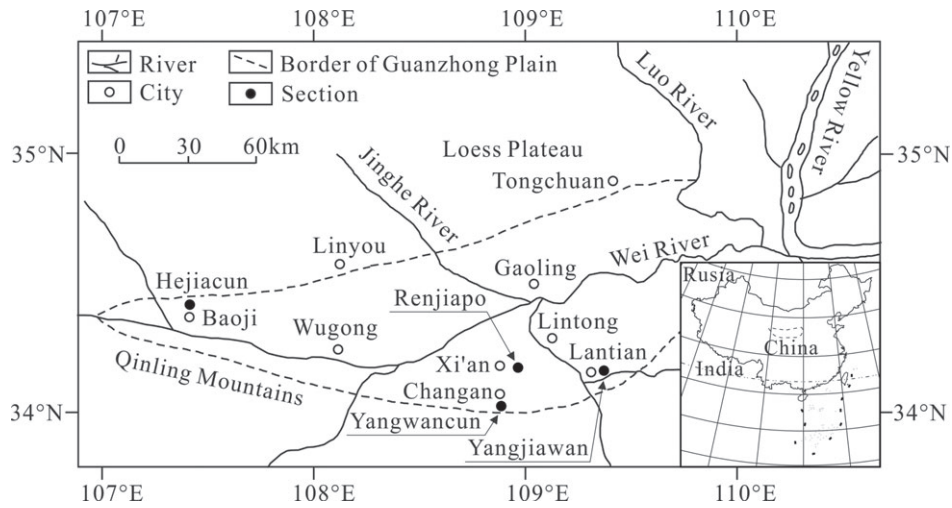


Figure 1 Locations of the study area and the profiles.

palaeo-humidity (Fedoroff & Glodberg, 1982; Guo & Liu, 1996) have been investigated, but there has been no attempt to quantify palaeo-water contents. Although soil structure in the Czech Republic and several humidity indices have been used in climate research (Kukla, 1977), information on palaeo water in palaeosols is very limited. The Quaternary loess and paleosol in South Korea formed under much stronger weathering conditions than in China (Hwang *et al.*, 2014). In Hungary, the variation in rainfall was large during the development of the loess and palaeosol (Schatz *et al.*, 2015). This research in South Korea and Hungary did not involve soil water contents, however.

Our review of existing work has shown that few direct signs of palaeo water in soil have remained, and that environmental indices that can be used to investigate soil–water relations are also limited. Although little information is available about palaeo-water–soil relations, it is important to expand the scope of Quaternary research to include this because the processes involve fundamental mechanisms controlled by the hydrological cycle and water balance. These issues are also relevant to both contemporary and future environmental change. Specific objectives of the present study were to characterize the S_1 palaeosol, to reconstruct soil water content and to relate that information to the climatic conditions at the time of the last interglacial.

Materials and methods

Profile sites

We observed and measured four S_1 palaeosol profiles in the Guanzhong Plain, and collected samples from three of them. The locations of these profiles are shown in Figure 1. The Yangjiawan profile (34°10'N,109°18'E) was recorded from the second terrace of the Ba River, ~1 km to the east of Lantian, which is a county administered by Xi'an. The Yangwancun profile (34°05'N, 108°58'E) was taken from the western slope of the Shaoling Tableland, which is ~10 km to the south of Xi'an. Finally, the

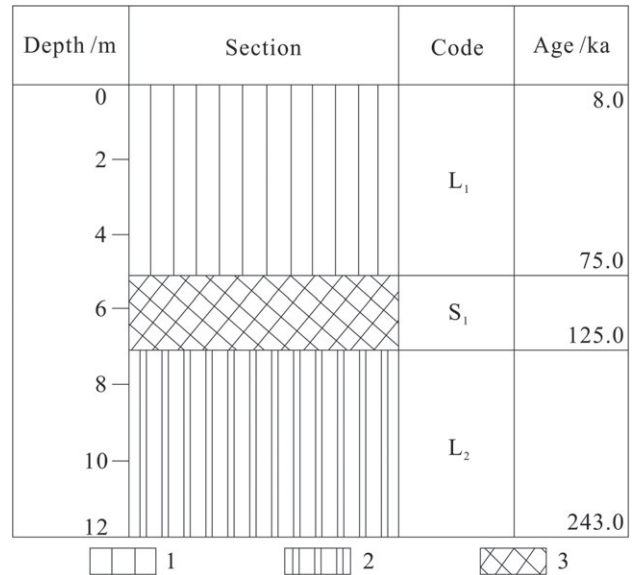


Figure 2 Distribution of S_1 palaeosol in the loess profiles. L₁, first loess layer; L₂, second loess layer; S₁, first palaeosol layer.

Hejiacun profile (34°23'N,107°07'E) was from the north slope of the Ling Tableland, ~2 km to the north of Baoji.

General situation and strata of the area studied

A temperate monsoon climate prevails in the region: the mean annual temperature is ~13°C and mean annual precipitation ~600 mm. Profiles in this area were complete; the thickness of loess from the early Pleistocene to Holocene is about 120 m. The S_1 palaeosol is about 1.8-m thick; it lies below the L₁ loess and above the L₂ loess (Figure 2). The thicknesses of L₁ and L₂ loess are about 5.0 and 4.5 m, respectively (Figure 2). Previous research (Liu, 1985; Guo & Liu, 1996) suggested that the ages of the lower bound of

the L₂ loess and S₁ palaeosol are 243.0 and 125.0 ka, respectively, and the ages of the lower and upper bounds of L₁ loess are 75.0 and 8.0 ka, respectively (Figure 2). Therefore, development of the S₁ palaeosol continued for about 50 ka.

Sampling and experiment

The upper part of the L₂ loess was leached during development of the S₁ palaeosol; the S₁ palaeosol and L₂ loess provided the materials for this study.

Samples were collected at 5-cm intervals from the Bt layer (a mineral horizon enriched in clay, in this case a reddish-brown (7.5 YR) argillic layer, the leached loess layer and an illuvial horizon of CaCO₃). In total, 232 samples were collected. In addition, 18 samples were taken to determine porosity at 20-cm intervals from the Renjiapo profile in Xi'an. An Axios advanced PW4400 X-ray fluorescence (XRF) spectrometer was used for determining the concentrations of selected elements. For the XRF analyses, the samples were first dried, then ground and sieved through a 200-mesh screen. The samples were then pressed into pellets before the above analysis. All element concentrations were corrected for carbonate, which in turn was quantified by a volumetric method (Zhao *et al.*, 2014). The soil microstructure was characterized with a scanning electron microscope and optical microscopy, and the chemical composition of those samples was determined by energy dispersive X-ray spectroscopy (EDX). The sample was sprayed with gold first before using the electron microscope to identify soil microstructure. The sample was processed into slides of 0.03-mm thickness before optical microscopy to identify soil microstructure. Analysis of the gases in the sample was used to determine CaCO₃ content. Porosity of the soil (%) was calculated from bulk density and the particle density of soil by the following equation (Hu & Yang, 1984):

$$\text{Porosity} = 100 (1 - \text{bulk density}/\text{particle density}).$$

The particle density of loess is 2.7, and of the S₁ palaeosol it is 2.75 (Hu & Yang, 1984). Particle-size composition was determined with a laser grain analyser (Mastersizer 2000, Malvern Instruments, Malvern, UK). When soil particle-size composition was analysed, the CaCO₃ in soil samples was first dissolved by hydrochloric acid. The clay in samples was then decomposed by sodium hexametaphosphate, and finally samples were analysed by the laser grain analyser. Analytical methods used to quantify basic soil properties for the WRB classification are from the ISSS Working Group Reference Base (1998). The samples were prepared and analysed at the Institute of the Earth Environment of the Chinese Academy of Science and the Environmental Laboratory of Shaanxi Normal University, Xi'an City.

Results

Subdivisions of S₁ palaeosol profiles

The S₁ palaeosols from all four profiles were well developed and had clear macroscopic horizontal zonation. Field observations show

Table 1 Stratification of S₁ palaeosol sections from the Guanzhong Plain

Soil section site	Bt horizon Thickness / m	Bc horizon Thickness / m	Cl horizon Thickness / m	Ck horizon Thickness / m	Red ferri-argillans Thickness / m
Yangjiawan, Lantian	1.8	1.0	1.2	4.0	2.8
Renjiapo, east of Xi'an	1.9	1.1	1.2	4.2	2.9
Yanwancun, south of Xi'an	2.0	1.2	1.1	4.3	3.0
Hejiacun, Baoji	1.8	1.2	1.4	4.4	3.0

that the Quaternary loess section in the study area is extensive; the thickness of loess from the early Pleistocene to Holocene is ~120 m, and thickness of the S₁ argillic horizon is 1.8 m. Argillans in the S₁ palaeosols are well developed in the Bt horizon (Figure 3a–d) and also occur in the weathered and leached loess layer (Figure 3a,b; Bc and Cl horizon), which is ~2.2-m thick beneath the Bt horizon (Figure 3a,b, Table 1).

The S₁ palaeosol profiles we examined are similar in many ways to each other (Table 1), and they can be divided into four horizons (Figure 3a,b). The first of these is a reddish-brown (7.5 YR) argillic horizon (Bt), which is intensely weathered, shows well-developed ferri-argillans and is 1.8–2.0-m thick. The second layer (Bc) is a weathered and leached loess layer ~1-m thick that contains ferri-argillans, most of which are distributed along root passages. The horizon boundaries between Bt and Bc are diffuse. The third layer (Cl) is a weathered and leached loess layer (1.1–1.4-m thick) that does not contain reddish brown (7.5YR) ferri-argillans and has large fissures along which leaching occurred; the Bc and Cl horizons grade into one another gradually. The fourth layer (Ck) is an illuvial horizon in the loess that marks the horizon with CaCO₃ concretions; it is ~2 m beneath the Bt horizon and is 0.2–0.3-m thick.

Observations of the S₁ palaeosol profiles from Yangjiawan, Yanwancun and Hejiacun show that the CaCO₃ illuvial horizon is not at the bottom of the argillic horizon (Bt), but at a depth of ~2 m in the weathered and leached loess layer under the argillic horizon (Figure 3a,b). The CaCO₃ illuvial horizon is stable and ~0.2-m thick, and is composed of CaCO₃ nodules ~10–15 cm in length and greyish-white (N9) in colour. In the upper ~0.6 m of the layer, there are numerous CaCO₃ films that are distributed over the surface of the fractured argillic horizon, which are prismatic in structure (Figure 3e,f).

Element and particle-size analysis of the S₁ palaeosol

The results from the chemical analysis (Figure 4, Table 2) in the S₁ palaeosol of Yanwancun show that the mean concentrations of Fe₂O₃, Al₂O₃ and SiO₂ in the Bt horizon are 5.95, 13.74 and 56.49%, respectively. This is 0.87, 1.72 and 3.04% more than in the parent loess horizon (C horizon), respectively, but concentrations of CaO and Na₂O are smaller than in the parent loess horizon (Figure 4, Table 2). The concentrations of Fe₂O₃, Al₂O₃, SiO₂, CaO and Na₂O in the Bc and Cl horizons are slightly smaller than those in

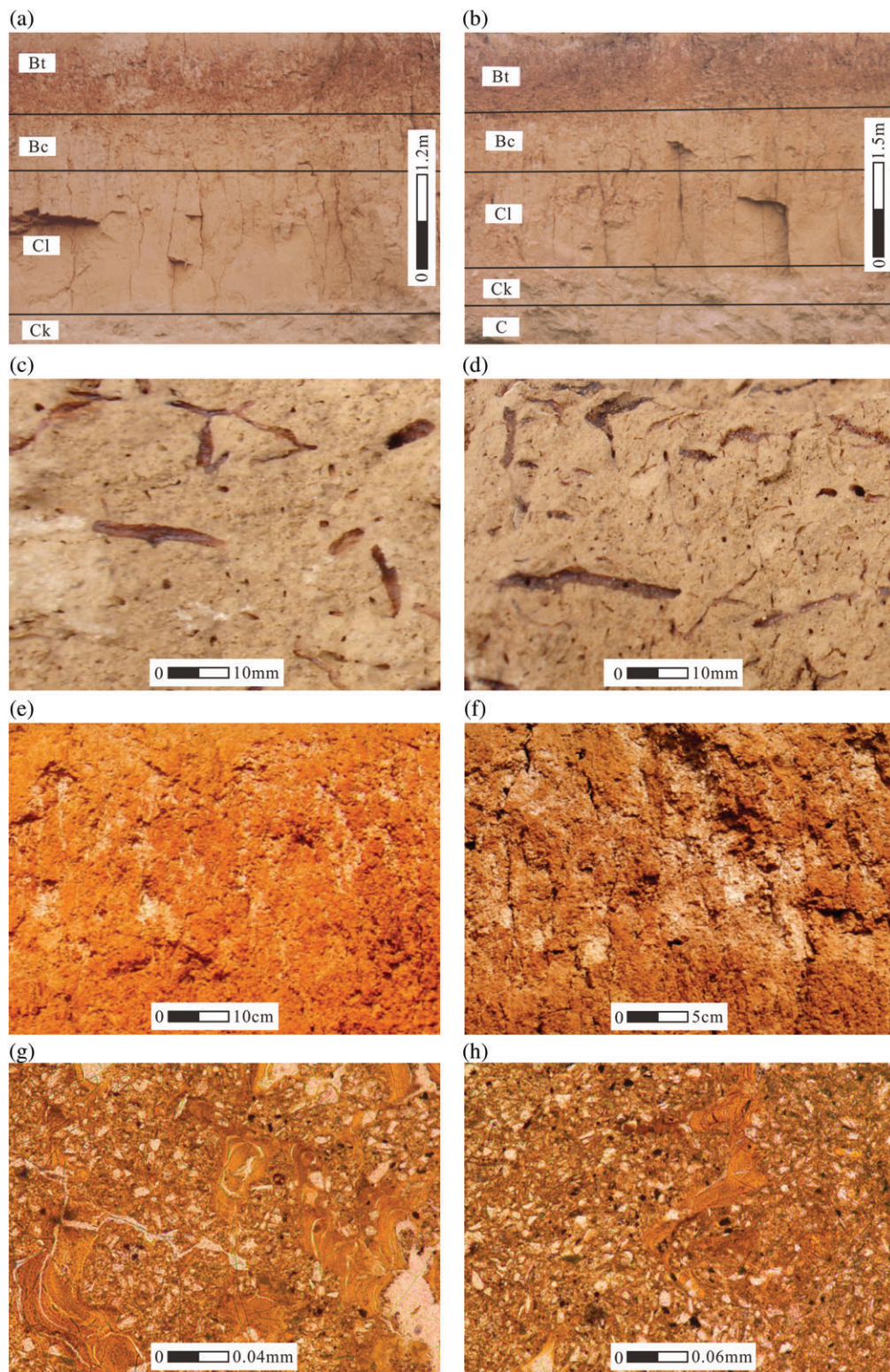


Figure 3 Stratification and microstructure of the S_1 palaeosol sections: (a, b) Hejiacun and Yangjiawan profiles, (c, d) distribution of red ferri-argillans in weathered and leached loess at Hejiacun and Yangjiawan, (e, f) numerous greyish-white $CaCO_3$ films in the upper Bt horizon of the S_1 palaeosol in the Renjiapo and Yangjiawan profiles, respectively. Bt, argillic horizon of paleosol; Bc, weathered and leached loess layer with thin flakes and spot ferri-argillans; Cl, weathered and leached loess layer without spot argillans; Ck, illuvial layer of $CaCO_3$; C, the parent loess without weathering.

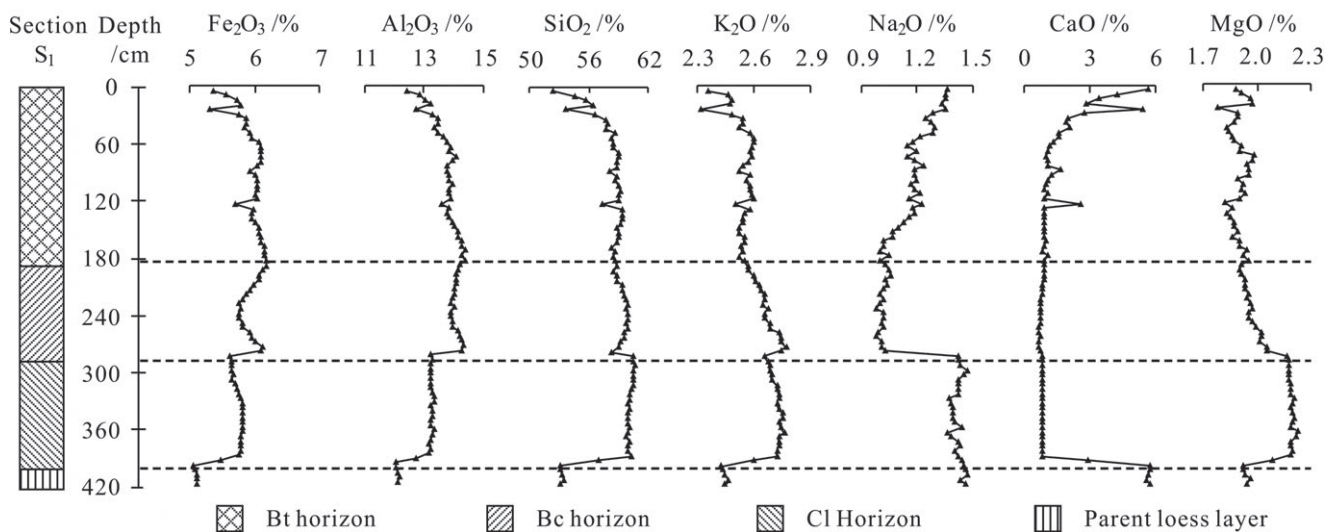


Figure 4 Change of chemical concentrations in the S₁ palaeosol section of the Yangwancun profile.

Table 2 Main oxide content and weathering index in the Yangwancun profile

Oxide	Bt horizon		Bc horizon		Cl horizon		C horizon	
	Range / %	Mean / %	Range / %	Mean / %	Range / %	Mean / %	Range / %	Mean / %
Fe ₂ O ₃	5.33–6.17	5.95	5.61–6.17	5.92	5.49–5.83	5.75	4.91–5.13	5.08
Al ₂ O ₃	12.45–14.39	13.74	13.23–14.35	14.05	12.75–13.35	13.23	11.84–12.20	12.06
SiO ₂	52.42–59.42	56.49	58.36–59.97	59.39	55.48–60.66	59.96	50.94–57.01	53.45
K ₂ O	2.31–2.59	2.53	2.56–2.76	2.66	2.59–2.75	2.71	2.34–2.45	2.41
Na ₂ O	1.00–1.36	1.12	0.98–1.42	1.04	1.36–1.45	1.41	1.43–1.47	1.45
CaO	0.89–5.68	1.69	0.71–0.95	0.81	0.83–2.96	0.95	5.61–7.43	6.01
MgO	1.78–1.98	1.90	1.90–2.17	1.98	2.09–2.23	2.19	1.87–1.96	1.92
Index	57.00–76.50	71.98	75.40–76.20	75.90	72.50–73.00	72.70	51.40–64.60	56.40

Index in the table is weathering index.

the Bt horizon (Figure 4, Table 2). The chemical composition shows that the Bt, Bc and Cl horizons are clearly weathered.

Based on the grain size analysis of the S₁ palaeosol in Yangwancun, the particle size is mainly less than 0.005 mm (Table 3); the next important size fraction is silt. The average particle-size composition of each layer is different. The argillic horizon (Bt layer) has the largest clay content, followed by the Bc and Cl layers. Clay content is smallest in the parent loess layer; the average content here is about 13% less than in the argillic horizon (Table 3).

The CaCO₃ content in the S₁ palaeosol

Results of gasometric analyses show that the CaCO₃ concentrations in most parts of the three profiles are very small, and the variation in CaCO₃ with depth is also mostly small (Table 4, Figure 5). The CaCO₃ content is in general 0–1.5% from the middle of the argillic horizon to the bottom of the weathered-fractured loess horizon, but it is slightly larger, from 0.2 to 8.9%, in the upper 30 cm of the argillic horizon. The CaCO₃ concentration is large, from 40 to 60%, in the CaCO₃ illuvial horizon.

Leaching fractures and weathered loess horizons in the S₁ palaeosol profiles

Field observations show that microfissures developed not only in the argillic horizon of the S₁ palaeosol in profiles from the Bailu, Shaoling and Ling Tablelands, but also in the middle–upper part of the underlying loess (L₂) (Figure 3a,b). The characteristics of the fractures vary with depth: those in the upper parts of the profiles are relatively dense with intervals between them of ~10 cm, whereas the lower fractures are relatively thin with larger intervals of 20–30 cm.

Well-developed fractures exist from the bottom boundary of the argillic horizon to the upper boundary of the CaCO₃ illuvial layer (Figure 3a,b); they differ from the original vertical joints. First, the leaching fractures are relatively dense and their density is greater than the original fractures in the loess layer; the leaching fractures were formed by strong eluviation and adhesive action of loess. Second, the fracture density changes with depth, decreasing from the top to the bottom of the weathered loess horizon; this was caused by more eluviation in the upper part of the layer than at the

Table 3 Composition of particle sizes in the S₁ palaeosol of Yangwancun

Layers	< 0.005 mm		0.005–0.01 mm		0.01–0.05 mm	
	Range / %	Mean / %	Range / %	Mean / %	Range / %	Mean / %
Bt	67.82–78.91	73.41	18.17–21.50	19.84	6.17–9.28	6.04
Bc	65.10–79.05	69.37	19.04–24.13	21.49	7.31–10.05	8.30
Cl	61.46–72.48	67.25	20.73–25.10	23.16	7.42–12.74	8.27
C	54.18–64.51	60.54	24.32–31.06	27.43	8.59–14.17	11.01

Table 4 The CaCO₃ and Sr concentrations in S₁ in Guanzhong Plain

Type	Layer	Yangjiawan profile		Hejiacun profile		Yangwancun profile	
		Content range	Mean	Content range	Mean	Content range	Mean
CaCO ₃ / %	Bt	0–7.6	1.8	0–8.2	2.1	0–8.9	2.5
	Bc	0–0.9	0.4	0–0.7	0.5	0–0.6	0.3
	Cl	0–1.3	0.8	0–1.5	0.7	0–0.9	0.5
	Ck	46.3–67.7	61.6	44.1–54.7	52.4	28.7–43.8	36.3
Sr / 10 ⁻⁶	Bt	174.3–188.4	180.2	174.3–202.9	183.8	102.6–125.2	109.4
	Bc	104.3–208.7	162.6	147.1–177.5	159.9	114.7–129.8	123.1
	Cl	163.3–214.7	182.7	143.6–153.4	150.4	128.3–147.7	136.9
	Ck	180.3–224.7	212.8	220.2–219.1	223.3	150.3–167.5	156.3

bottom. Third, the distribution of the leaching fractures is controlled by the eluvial horizon; this type of fracture does not exist in the unweathered and unleached loess layer below the illuvial CaCO₃ horizon.

Beneath the S₁ there are weathered loess layers that do not exist under most of the other palaeosol layers (Figure 3; Bc layer, Cl layer). The weathered loess horizon has three obvious characteristics. First, it shows evidence of the eluviation of CaCO₃ as the S₁ developed. Second, the loess layer is slightly more yellow and red because of oxidation; this was probably caused by the relatively high ambient air temperatures and rainfall during the development of S₁. Third, leaching fractures exist in the weathered loess horizons; these relate to palaeo-moisture content as discussed below.

Distribution of ferri-argillans and microstructures in the S₁ palaeosol

Field observations indicate that the red argillans developed in the argillic horizon of the S₁ palaeosol, but smaller amounts of reddish-brown (7.5 YR) ferri-argillans also occur ~1 m below that horizon (Figure 3a–d). The ferri-argillans that developed on particles in the argillic horizon appear as bright films; they also occur ~1 m beneath that layer in slender empty channels with spot-like or linear forms (Figure 3a–d). The reddish-brown (7.5 YR) ferri-argillans migrated ~1 m into the loess, and this provides convincing evidence for the migration of the ferruginous components out of S₁.

Five samples of the material in the ferri-argillans were examined with the scanning electron microscope (SEM), which showed that

the ferri-argillans have two types of pattern. One type has minimal clay mineral crystals (Figure 6a,b) with obvious directional alignment. The other type of ferri-argillan comprises uncrystallized fine clay and Fe₂O₃ with colloidal morphologies with typically spherical or amorphous shapes (Figure 6c,d).

Observations by an optical microscope of 36 thin-sections from Bt horizons in the three S₁ profiles showed that argillans with strong optical properties developed well. They mostly form irregular lumps and flow structure is clear (Figure 3g,h). The argillans with strong optical properties can indicate soil moisture content, as described below in the discussion.

The EDX analysis (Table 5, Figure 7a–d) shows that Fe₂O₃ and Al₂O₃ account for 12–16 and 23–26% of the ferri-argillan mass, respectively. The material observed by SEM and the argillans analysed by EDX is insoluble clay matter.

Strontium content and migration from the S₁ palaeosol

The characteristics of Sr and Ca are similar; Sr migration in the soil profile is usually very obvious and can indicate the palaeo environment (Chen *et al.*, 2006a).

Concentrations of Sr (Figure 8, Table 4) in the three profiles studied vary from 110 to 240 µg g⁻¹ and show distinct distributional differences in the various strata. Changes in Sr concentrations can be used to divide the profiles into five layers. The Sr content in the first layer (of 0–0.5-m depth in the palaeosol layer) is relatively large and corresponds to the upper part of the argillic horizon. Field observations indicated that large quantities of white CaCO₃ films also occur in this part of the palaeosol, and the large Sr content can be explained by the migration of Sr from the overlying loess

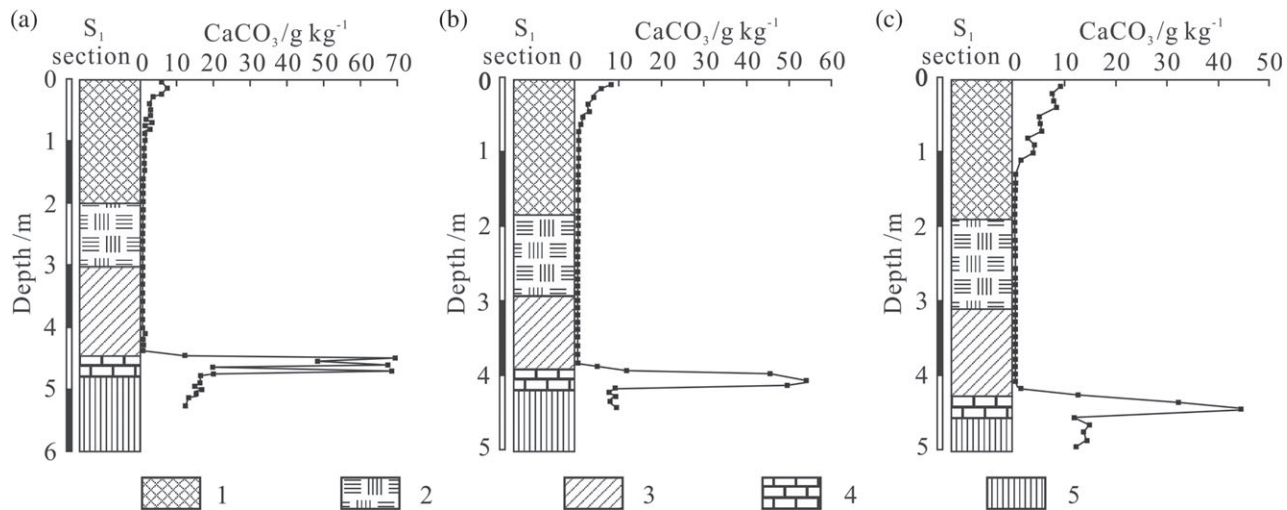


Figure 5 Variation in CaCO_3 content in a section of the S_1 palaeosol from the Guanzhong Plain: (a) Hejiacun, (b) Yangwacun and (c) Yangjiawan profiles. Key to fill patterns: 1, palaeosol; 2, weathered and leached loess layer with red ferri-argillans; 3, weathered and leached loess layer without red ferri-argillans; 4, illuvial horizon of CaCO_3 ; 5, unweathered loess.

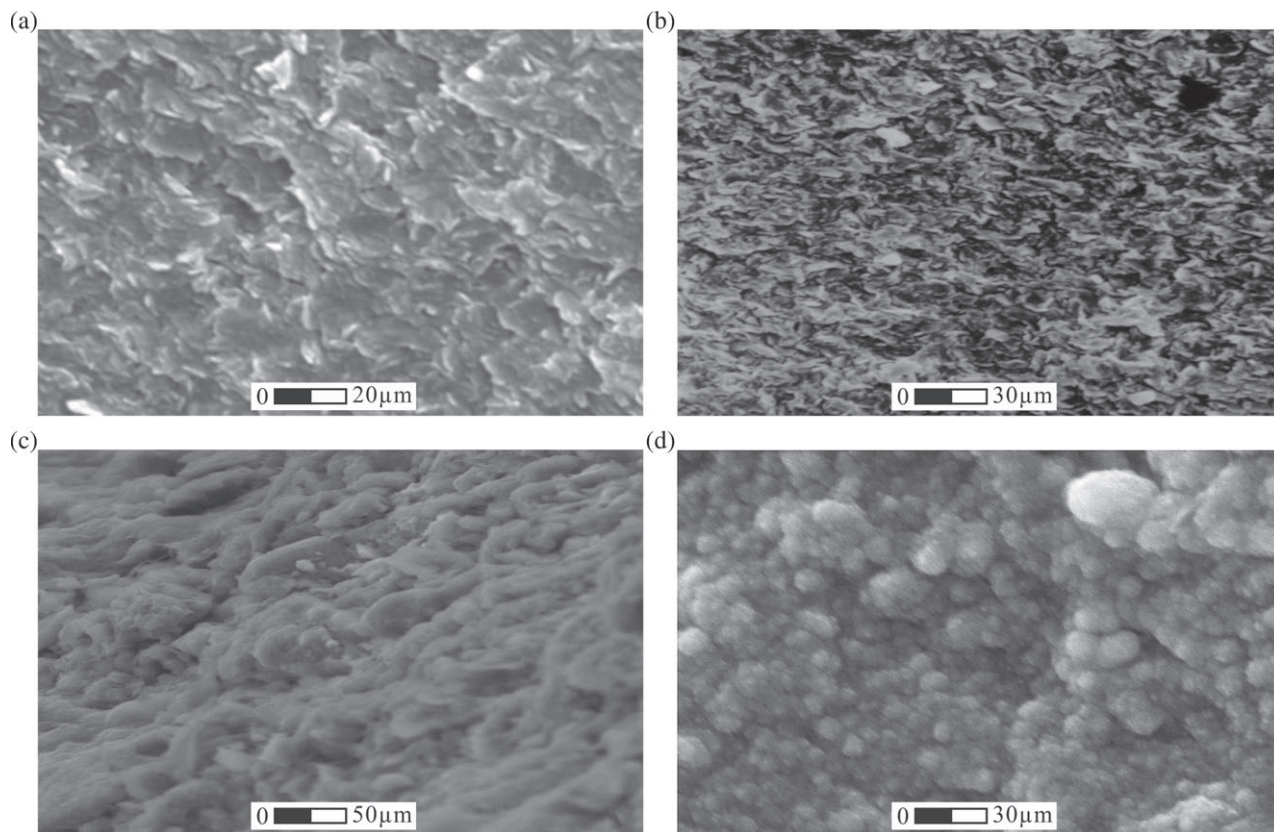
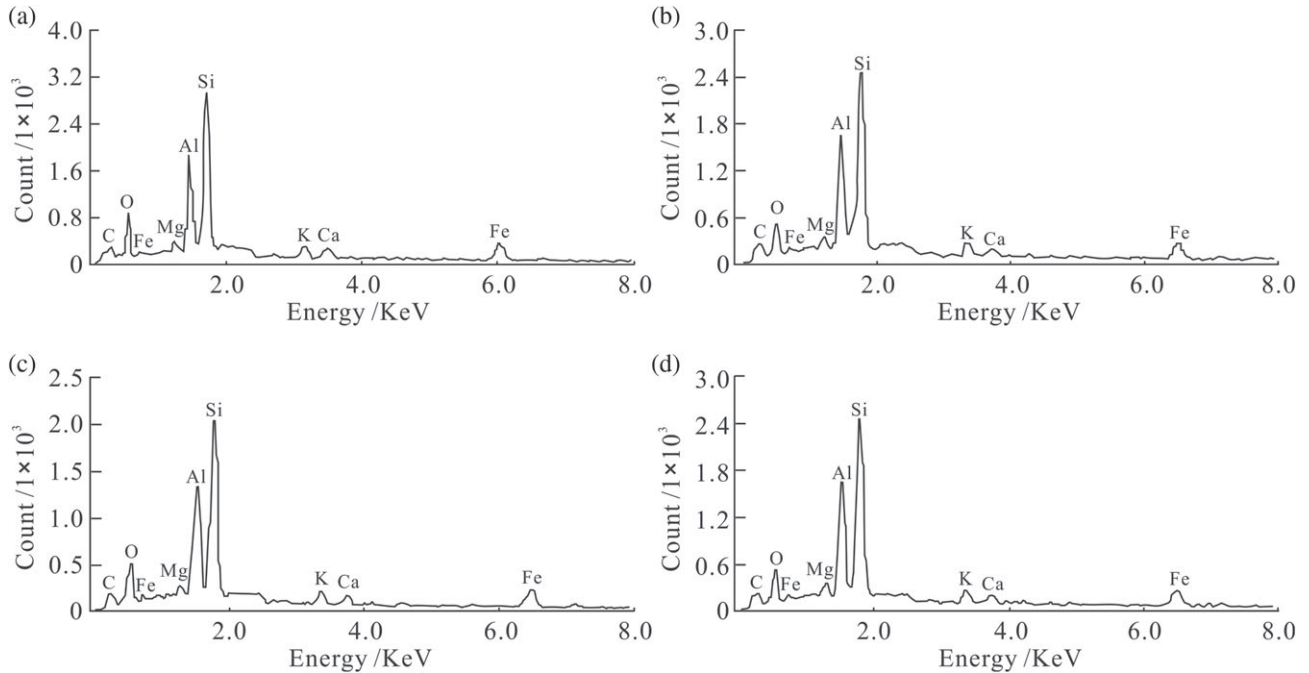


Figure 6 Forms of red ferri-argillans in the S_1 palaeosol from the Guanzhong Plain. Microcrystals of clay minerals in the argillans under the S_1 palaeosol at (a) Yangwacun and (b) Hejiacun. Ferri-argillans with colloidal morphologies in the S_1 palaeosol from (c) Yangjiawan and (d) Hejiacun.

Table 5 Chemical constituents of ferri-argillans in the S_1 palaeosol from Guanzhong Plain

Sites	Sample number	SiO ₂ / %	Al ₂ O ₃	Fe ₂ O ₃	K ₂ O	MgO	CaO
Yangjiawan	X01	53.4	23.8	15.4	2.3	2.1	2.9
Yangwancun	X02	53.4	24.8	13.0	3.3	2.6	2.1
Hejiacun	X03	53.3	25.1	12.9	3.3	2.7	2.7
Hejiacun	X04	54.1	24.8	13.0	3.3	2.6	2.8
Yangwancun	X05	53.9	23.4	15.3	3.0	2.4	2.2

**Figure 7** Energy spectra of argillans from the S_1 palaeosol in Guanzhong Plain. Element composition of argillans from the S_1 palaeosol from (a) Yangjiawan, (b) Yangwancun and (c, d) Hejiacun profiles.

layer (not shown). The second layer at a depth of 0.5–2.2 m in the palaeosol–loess profile corresponds with the middle and lower parts of the argillic horizon. The Sr content in the second layer is the smallest of the five layers (Figure 8), indicating that Sr was transported out of this layer. The third layer is 2.2–4.0 m from the top of S_1 and its depth varies among the profiles, but corresponds to the leached loess horizon. The Sr content of the third layer is larger than that of the first two layers of the Yangjiawan and Hejiacun profiles. The Sr concentrations in the third layer are smaller than those in the second layer of the Yangwancun profile (Figure 8). They increase from the upper to lower part of the third layer in each profile; this is evidence for Sr migration. The fourth layer, from 4.0 to 4.3 m in the palaeosol profiles, corresponds to the CaCO₃ illuvial horizon and has the largest Sr content of the five layers (Figure 8). The Sr concentration in the horizon with CaCO₃ concretions is very large, presumably because of illuviation and accumulation of Sr in the CaCO₃. The fifth layer, below 4.0–4.3 m in the profiles, corresponds to the loess parent material below

the CaCO₃ illuvial horizon. The Sr concentration in layer five is relatively large, but slightly less than that of the CaCO₃ illuvial horizon.

All the results and observations described above indicate that Sr had leached and migrated in the profiles, and there are hierarchical characteristics in the palaeosol profile. The general order of Sr concentrations is Ck > C (parent material layer) > Cl > Bt > Bc horizons. The Sr content in the Bt horizon is probably less than in the Bc and Cl horizons because the Bt horizon is argillic and a fraction of the Sr would have been adsorbed by clay minerals. The Sr data for the profile suggest a migration depth similar to or the same as that of CaCO₃, ~4.0 m.

Porosity in the S_1 palaeosol profile

Results of the determination of porosity (Table 6) show that it varies between 43.84 and 47.28% (the average is 45.71%) in the argillic horizon of the S_1 palaeosol in Yangwancun. The porosity in weathering–leaching loess horizons (Bc and Cl horizon) varies

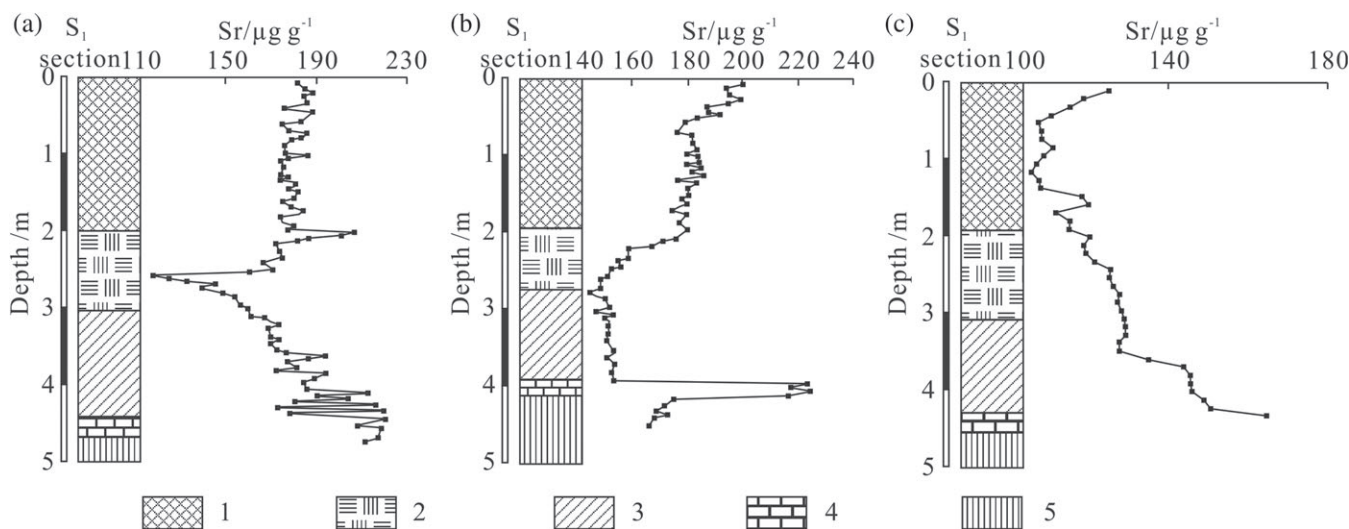


Figure 8 Variation in Sr concentrations in sections of the S_1 palaeosol from the Guanzhong Plain: (a) Hejiacun, (b) Yangwancun and (c) Yangjiawan profiles. Key to fill patterns: 1, palaeosol; 2, weathered and leached loess layer with red ferriferous argillans; 3, weathered and leached loess layer without red ferriferous argillans; 4, illuvial horizon of CaCO_3 ; 5, unweathered loess.

Table 6 Porosity in the S_1 palaeosol profile of Yangwancun (%)

Layer	Bt	Bc	Cl	C
Content range / %	43.84–47.28	46.39–49.13	48.26–49.02	48.26–50.14
Mean content / %	45.92	47.34	48.30	49.19
Sample number	9	5	4	5

between 47.39 and 50.73% (the average is 48.93%); this is about 3% less than that in the argillitic horizon.

Discussion

Soil type and weathering stage of S_1 palaeosol

The argillitic horizon of the S_1 palaeosol is well developed (Figure 3a,b, Table 3); it has new argillans with optical properties (Figure 3g,h), newly formed clay minerals (Figure 6) and shows clear evidence of the migration of Fe_2O_3 and CaCO_3 (Figure 5). It is known that the S_1 was subject to a strong chemical weathering process and was an eluvial soil. The migration of Fe_2O_3 occurs under acidic conditions, indicating that development of the palaeosol reached the acid leaching stage. Compared with other soils in the world, the S_1 palaeosol is equivalent to a Luvisol in the soil classification system (ISSS Working Group Reference Base, 1998).

There are many indices for determining the strength of weathering of a soil (Nesbitt & Young, 1982; Brahy *et al.*, 2000; Chadwick *et al.*, 2003). The chemical weathering index (CIA) was used here to determine the degree of weathering of the S_1 palaeosol. The CIA (%) is calculated by the following formula:

$$\text{CIA} = \left[\frac{\text{Al}_2\text{O}_3}{(\text{Al}_2\text{O}_3 + \text{CaO} + \text{Na}_2\text{O} + \text{K}_2\text{O})} \right] \times 100,$$

where CaO represents the CaO in silicate minerals only in the formula. The results of the calculations with this formula are given in Table 2. In the S_1 palaeosol of Yangwancun, the average CIA of the Bt, Bc, Cl and C layers is 72.0, 75.9, 72.7 and 56.4%, respectively. According to the study by Nesbitt & Young (1982), CIA values between 50 and 65% reflect a low degree of chemical weathering in a cold and dry climate, whereas a CIA between 65 and 85% reflects moderate chemical weathering under warm and humid conditions and a CIA between 85 and 100% reflects strong chemical weathering under hot and humid tropical and subtropical conditions. Therefore, the Bt, Bc and Cl horizons of S_1 were subjected to moderate chemical weathering under warm and humid climate conditions.

Gravitational and available water content during development of the S_1 palaeosol

The vertical zonation from soil water to groundwater is generally divided into three zones, namely gravitational, adsorbed and underground water (Huang *et al.*, 1998). Adsorbed water in soil is that adsorbed on the surface of soil particles by adhesion. Gravitational water is the water that moves through soil under the influence of gravity (Huang *et al.*, 1998; Yang & Shao, 2000). Less than 20% of the soil water in the Guanzhong Plain is adsorbed and more than 20% is gravitational water (Yang & Shao, 2000).

From field observations and laboratory analysis, we found that three types of data are useful for understanding water content and water zonation; these are (i) the migration depth of CaCO_3 and Sr, (ii) the depth of weathered and leached loess horizons and (iii) the migration depth of ferri-argillans. We propose that it is gravitational water that causes the chemical constituents in the soil to dissolve and migrate. Previous researchers have suggested that adsorbed water could dissolve the soluble

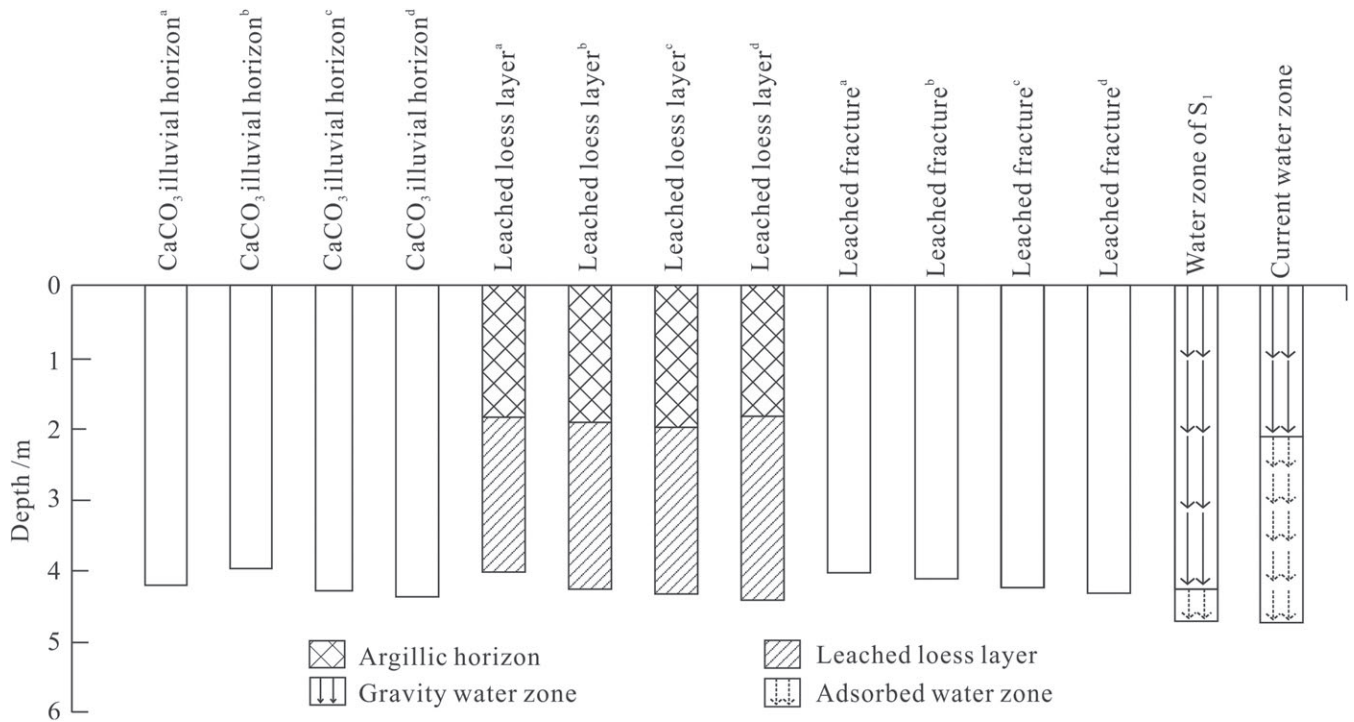


Figure 9 The depth of gravitational water and adsorbed water during development of the S_1 palaeosol on the Guanzhong Plain. The index of zonation of gravitational water from the profiles at (a) Yangjiawan, (b) Renjiapo, (c) Yangwancun and (d) Hejiacun.

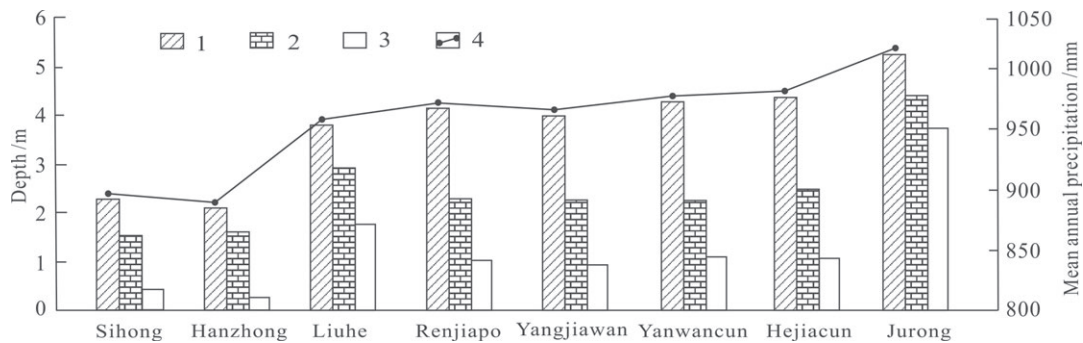


Figure 10 Relation between climate indices and mean annual precipitation of the S_1 palaeosol and yellow-brown forest soil. The bar charts for Sihong, Liuhe and Jurong in Jiangsu and Hanzhong in Shannxi represent the profile horizon thickness of modern subtropical yellow-brown forest soil. The bar charts for Yangjiawan, Yangwancun and Hejiacun represent the thickness of the S_1 palaeosol layer. Key to fill patterns: 1, migration distance of the $CaCO_3$ illuvial horizon from the upper boundary of the argillic multi-fracture horizon and the lower boundary of the illuvial horizon of $CaCO_3$ concretions; 2, migration distance of Fe_2O_3 from the bottom boundary of the argillic horizon to the lower boundary of red argillans; 3, thickness of the weathered and leached loess horizon; 4, the average annual precipitation curve.

salts, but the process has been found to be slow (Huang *et al.*, 1998). Results from some of our earlier research showed that adsorbed water can dissolve soluble salts but only negligible amounts of carbonate, and that this type of water migrates slowly and does not cause $CaCO_3$ to precipitate (Zhao, 2003; Zhao *et al.*, 2014).

From measurements of the depth of gravitational water in Xi'an, Luochuan and Changwu in 2003 (Chen *et al.*, 2006a; Liu *et al.*, 2010; Zhao *et al.*, 2011), which was a wet year, we can conclude that when S_1 developed, the depth of gravitational water should have

been at the lower boundary of the $CaCO_3$ illuvial layer. In the three S_1 profiles, the lower boundary depth of $CaCO_3$ and Sr migration is 4.2 m from the top of S_1 , indicating that gravitational water reached at least that depth (Figure 9).

The leaching fractures in the weathered loess horizon resulted in the migration of soluble components and the transport of colloidal Fe_2O_3 . Transport is favoured in soils with large gravitational water contents (Zhao *et al.*, 2014). These fractures extend downwards from the top of the palaeosol to the upper boundary of the Ck horizon (Figure 3a,b), a depth of ~ 4 m. Therefore, the weathered

Table 7 Migration depth of CaCO₃ and Fe₂O₃, thickness of weathered parent loess and climate of S₁ palaeosol and modern subtropical soils

Sites	Yangjiawan	Yangwancun	Hejiacun	Sihong	Liuhe	Jurong
Soil or palaeosol	S ₁	S ₁	S ₁	Ye	Ye	Ye
Migration depth of CaCO ₃ / m	4.0	4.3	4.4	2.2	3.4	4.5
Migration depth of Fe ₂ O ₃ / m	1.0	1.0	1.2	0.3	1.2	1.6
Thickness of weathered parent loess / m	2.2	2.3	2.6	0.3	2.0	3.0
Mean annual precipitation / mm	1000	1000	1100	890	1050	1100
Mean annual temperature / °C	16	16	16	15	16	16

Migration depth of CaCO₃ refers to vertical distance between the upper boundary of the Ck horizon and the upper boundary of the Bt horizon. Migration depth of Fe₂O₃ refers to vertical distance between the upper boundary of distribution of red ferri-argillans and the lower boundary of the Bt horizon. Ye represents modern subtropical yellow-brown forest earth.

and leached loess horizons also indicate that gravitational water reached a depth of at least 4 m (Figure 9).

The argillans (Figures 3g,h, 6) with optical properties are well developed in the S₁ palaeosol, and the formation of the argillans required soil water content to be close to saturation (Fedoroff & Glodberg, 1982; Guo & Liu, 1996). The porosity of the Bt horizon in the S₁ palaeosol is about 46% (Table 6), which shows that palaeo-moisture content in the Bt horizon was about 46% in the rainy season.

The gravitational water content in modern silt soils from the Guanzhong Plain and the Loess Plateau at depths of 0–4.2 m is ~22% during the growing seasons of rainy years (Liu *et al.*, 2010; Zhao *et al.*, 2011). This can be taken as an approximation of the gravitational water content during the period of S₁ development. Although gravitational water becomes adsorbed water as sorption proceeds, the change occurs gradually and adsorbed water in the soil is still large, usually ~16% over a depth range of 4.3–6.0 m (Chen *et al.*, 2006a; Liu *et al.*, 2010; Zhao *et al.*, 2011). This suggests that when S₁ developed, the soil water content was large between 0 and 6 m (Figure 9).

Total soil moisture includes both available water and water tightly sorbed to particles, which is unavailable and called ‘bound’ water (Yang & Shao, 2000). The latter cannot be absorbed and utilized by plants, thus the term ‘available water’ refers to the total soil water content minus the bound water. In the Guanzhong Plain, the bound water content of loess is ~8% (Yang & Shao, 2000; Zhao *et al.*, 2011). Assuming a total soil water content of 22%, which is the average from 0 to 4.2 m as discussed above, one can show that the available water content after all kinds of consumption during the development of the S₁ palaeosol was ~14%.

Studies of carbon isotopes have led some researchers to suggest that the biomes were mainly grasslands and forest-steppes in Lantian from 800 ka (Lin & Liu, 1992). A large soil water content of 22% indicates that broad-leaved forests probably dominated the plant communities during the development of the S₁ palaeosol.

Climate during development of the S₁ palaeosol

The argillans of the S₁ palaeosol are reddish-brown in colour (Figure 3c,d), and this is a feature common to subtropical soils (Fedoroff & Glodberg, 1982; Guo & Liu, 1996). The rubefaction

of the soil presumably occurred when the ambient temperature and precipitation were both high because abundant precipitation favours mineral hydrolysis, and higher temperatures can accelerate rates of chemical reaction. Under warm and humid conditions, iron-containing silicates decompose to clay minerals and Fe₂O₃, which makes the soil appear red. According to a study by Xiong & Li (1987), there is no indication of rubefaction in semi-humid and semi-arid temperate areas of northern China because of the low temperatures and scant precipitation, but soils in southern China generally do develop the reddish colour.

The depths of migration of CaCO₃, red ferri-argillans, and the thickness of the weathered and leached loess horizons observed in the S₁ profile were greater than those in the modern Luvisols from Sihong and Liuhe in Jiangsu Province (Figures 3a–d, 10, Table 7), which are in the northern and the middle parts of the north subtropics, respectively (Xiong & Li, 1987). The depths of migration or of development of the four indicators in the S₁ profile were less than those in the modern Luvisols from Jurong with more precipitation (Figure 10, Table 7), which are in the southern part of the north subtropics (Xiong & Li, 1987). These macroscopic features observed are consistent with the experimental results of CaCO₃ and Sr contents, and so we can conclude that the climate during the development of S₁ was wetter than that of the Luvisols in Sihong and Liuhe.

The average annual temperature and precipitation at Liuhe at present are 15.1°C and ~990 mm, respectively (Xiong & Li, 1987). From this we can infer that the mean annual temperature on the Guanzhong Plain when the S₁ palaeosol developed was probably 15–16°C, and the mean annual precipitation was ~1000 mm. This suggests that the climate in our study area was subtropical when S₁ developed, and because of this, there can be little doubt that the Qinling Mountains did not act as a boundary between the subtropical and temperate climate zones at that time.

Water balance during the development of the S₁ palaeosol

Years of observations have shown that when the mean annual rainfall on the relatively flat Loess Plateau region is 600 mm, the total annual evaporation and precipitation for woodland soils are roughly in balance (Yang & Shao, 2000); that is, evaporation, transpiration and canopy interception, as well as runoff, are almost equal to the rainfall (Yang & Shao, 2000).

On the other hand, the soil-water balance is positive when the annual rainfall is > 600 mm on the Loess Plateau. Conversely, the soil-water balance is negative when the average annual rainfall is < 600 mm (Yang & Shao, 2000). It is generally agreed that leached soils develop in areas where the mean annual precipitation is greater than the total annual water consumption (Xiong & Li, 1987).

Data presented above (Figures 3, 5, 8, Table 7) show that the S₁ palaeosol was strongly leached; therefore, the annual average rainfall was probably > 900 mm when S₁ developed. Furthermore, the annual average rainfall exceeded total water consumption when the S₁ palaeosol developed.

Studies of chemical migration in Chinese loess suggest that it is likely that the annual precipitation is greater than total water consumption when the CaCO₃ illuvial layer of a soil is more than 2 m deep (Xiong & Li, 1987; Zhao *et al.*, 2014). The CaCO₃ illuvial layer of the S₁ palaeosol developed at a depth of 4.2 m. This indicates that annual precipitation was considerably greater than total water consumption and that the water balance was positive when S₁ formed.

Conclusions

Weathered and leached loess layers and leached fractures, the depths of distribution of the illuvial CaCO₃ horizon, Sr and reddish-brown ferri-argillans provide important indicators of the palaeo-environment. They all provide information related to mean annual precipitation, soil water content and the depth of distribution of gravitational water when the S₁ palaeosol developed. Our analyses indicate that a subtropical climate prevailed in the Guanzhong Plain when the S₁ palaeosol developed. The moisture input to the soil was considerably more than that used or lost, and the water balance was positive at that time and provided enough water for forests to grow.

Acknowledgements

This research was funded by the National Natural Science Foundation (Grant No 41210002), the Project of Xi'an Geological Survey Center of China Geological Survey (Water [2016]4) and the State Key Laboratory of Loess and Quaternary Geology, Chinese Academy of Sciences (SKLLQG1626, SKLLQG1713). We also thank the editors and reviewers, whose suggestions and comments aided us in improving an earlier version of this manuscript.

References

- Bokhorsta, M.P., Beetsa, C.J., Markovic, S.B., Gerasimenko, N.P., Matviishina, Z.N. & Frechen, M. 2009. Pedo-chemical climate proxies in Late Pleistocene Serbian–Ukrainian loess sequences. *Quaternary International*, **198**, 113–123.
- Brahy, V., Titeux, H., Iserentant, A. & Delvaux, B. 2000. Surface podzolization in Cambisols under deciduous forest in Belgian loess belt. *European Journal of Soil Science*, **51**, 15–26.
- Bronger, A., Winter, R., Derevjanko, O. & Aldga, S. 1995. Loess-paleosol sequences in Tadjikistan as a palaeoclimate record of the Quaternary in central Asia. *Quaternary Proceedings*, **4**, 69–81.
- Chadwick, O.A., Gavenda, R.T., Kelly, E.F., Ziegler, K., Olson, C.G. & Elliott, W.C. 2003. The impact of climate on the biogeochemical functioning of volcanic soils. *Chemical Geology*, **202**, 195–223.
- Chen, J., Chen, Y., Liu, L.W., Ji, J.F., Balsam, W., Sun, Y.B. *et al.* 2006a. Zr/Rb ratio in the Chinese loess sequence and implication for changes in the East Asian winter monsoon strength. *Geochimica et Cosmochimica Acta*, **70**, 1471–1482.
- Chen, B.Q., Zhao, J.B. & Li, Y.H. 2006b. [Research of soil water character below artificial forest of the rainy year in Luochuan area of Yan'an.] *Arid Land Geography*, **29**, 532–536 (in Chinese).
- Fedoroff, N. & Glodberg, P. 1982. Comparative micromorphology of two Late Pleistocene paleosols (in the Paris Basin). *Catena*, **9**, 227–251.
- Gocke, M., Pustovoytov, K. & Kühn, P. 2011. Carbonate rhizoliths in loess and their implications for paleoenvironmental reconstruction revealed by isotopic composition: $\delta^{13}\text{C}$, ^{14}C . *Chemical Geology*, **283**, 251–260.
- Guo, Z.T. & Liu, D.S. 1996. Micromorphology of the loess-paleosol sequence of the last 130ka in China and Paleoclimatic events. *Science in China (Series D)*, **39**, 468–477.
- Guo, Z.T., Zhou, X. & Wu, H.B. 2012. Glacial-interglacial water cycle, global monsoon and atmospheric methane changes. *Climate Dynamics*, **39**, 1073–1092.
- Hu, G.T. & Yang, W.Y. 1984. *Engineering Geology*. Geological Publishing House, Beijing (in Chinese).
- Huang, X.Q., Li, H.M. & Jin, B.X. 1998. Groundwater types. In: Hydrology (eds X.Q. Huang, H.M. Li & B.X. Jin), pp. 232–242. Higher Education Press, Beijing (in Chinese).
- Hwang, S., Park, C.S., Yoon, S.O. & Choi, J. 2014. Origin and weathering properties of loess-paleosol sequence in the Goseong area on the east coast of South Korea. *Quaternary International*, **344**, 17–31.
- ISSS Working Group Reference Base 1998. *World Reference Base for Soil Resources*. World Soil Resources Report No 84, FAO, Roma.
- Jiang, Z.X. & Liu, Q.S. 2016. [Quatification of hematite and its climatic significances.] *Quaternary Sciences*, **36**, 676–668 (in Chinese).
- Kukla, G.J. 1977. Pleistocene land–sea correlations. *Earth Science Reviews*, **13**, 307–374.
- Lin, B.H. & Liu, R.M. 1992. The stable isotope evidence of summer monsoon evolution in the Loess Plateau during the latest 800 ka. *Chinese Science Bulletin*, **37**, 1691–1693.
- Liu, T.S. 1985. *Loess and Environment*. Science Press, Beijing (in Chinese).
- Liu, T.S. & Ding, Z.L. 1998. Chinese loess and the paleomonsoon. *Annual Review of Earth and Planetary Sciences*, **26**, 111–145.
- Liu, W.Z., Zhang, X.C., Dang, T.H., Zhu, Q.Y., Li, Z., Wang, J. *et al.* 2010. Soil water dynamics and deep soil recharge in a record wet year in the southern Loess Plateau of China. *Agricultural Water Management*, **97**, 1133–1138.
- Nesbitt, H.W. & Young, M. 1982. Early Proterozoic climates and plate motions inferred from major element chemistry of lutites. *Nature*, **299**, 715–717.
- Pecsi, M. 1997. Loess and other subaerial sequences in the middle Danubian basin. *Earth Science Frontiers*, **4**, 43–59.
- Peng, S.Z., Hao, Q.Z., Oldfield, F. & Guo, Z.T. 2014. Release of iron from chlorite weathering and links to magnetic enhancement in Chinese loess deposits. *Catena*, **117**, 43–49.

- Schatz, A., Scholten, T. & Kühn, P. 2015. Paleoclimate and weathering of the Tokaj (Hungary) loess-palaeosol sequence. *Palaeogeography, Palaeoclimatology, Palaeoecology*, **426**, 170–182.
- Sun, D.H., Wu, X.H. & Liu, D.S. 1996. Evolution of the summer monsoon regime over the Loess Plateau of the last 150 ka. *Science in China (Series D)*, **39**, 504–511.
- Xiong, Y. & Li, Q.K. 1987. *Chinese Soil*. Science Press, Beijing (in Chinese).
- Yang, W.Z. & Shao, M.A. 2000. Soil water form and water constant. In: *Study on Soil Moisture in Loess Plateau* (eds W.Z. Yang & M.A. Shao), pp. 67–83. Science Press, Beijing (in Chinese).
- Zhao, J.B. 2003. A pedocomplex and its paleoclimatic significance in Chinese Loess Plateau. *Soil Science*, **168**, 64–73.
- Zhao, J.B., Zhou, Q., Chen, B.Q., Du, J. & Wang, C.Y. 2011. Research of dynamic variation of moisture in apple orchard soil in the area of Xianyang in recent years. *Acta Ecologica Sinica*, **31**, 5291–5298 (in Chinese).
- Zhao, J.B., Cao, J.J., Jin, Z.D., Xing, S. & Shao, T.J. 2014. The fifth paleosol layer in the southern part of China's Loess Plateau and its environmental significance. *Quaternary International*, **334–335**, 189–196.